Solar Steam Reforming of Natural Gas for Hydrogen Production using Molten Salt Heat Carriers

Alberto Giaconia
ENEA Research Center "Casaccia", via Anguillarese, 301-00123 Rome, Italy

Marcello de Falco
Dept. of Chemical Engineering, University of Rome "La Sapienza", via Eudossiana, 18-00184 Rome, Italy

Giampaolo Caputo, Roberto Grena, and Pietro Tarquini
ENEA Research Center "Casaccia", via Anguillarese, 301-00123 Rome, Italy

Luigi Marrelli
Dept. of Chemical Engineering, University of Rome "La Sapienza", via Eudossiana, 18-00184 Rome, Italy

DOI 10.1002/aic.11510
Published online April 30, 2008 in Wiley InterScience (www.interscience.wiley.com).

The utilization of concentrated solar energy as external heat source for methane steam reforming has been investigated. Molten salts at temperatures up to 550°C can be used as solar heat carrier and storage system, and hydrogen selective membranes can be used to drive reforming reaction at lower temperatures than conventional (<550°C), with hydrogen purification achieved thereby. The combination of new technologies such as membranes and membrane reactors, concentrating solar power (CSP) systems, and molten salt heat carriers, allows a partial decarbonation of the fossil fuel together with the possibility to carry solar energy in the current natural gas grid. Different plant configurations and operating conditions have been analyzed using a mathematical model and AspenPlus simulator. © 2008 American Institute of Chemical Engineers *AIChE J,* 54: 1932–1944, 2008
Keywords: energy, green engineering, process simulation, membrane separations, hydrocarbon processing

Introduction

The needs to contain carbon dioxide emissions and the reduced availability of fossil fuels expected in the next years is leading to the progressively increasing exploitation of renewable and non-conventional energy sources worldwide.

The increasing hydrogen demand for hydrocracking and desulphurization operations in crude oil refinery, and its future growing use as energy carrier and storage medium make its production from renewables an important subject in the present and future energy policy. However, the pathway to hydrogen generation entirely from renewable energy and material sources reasonably goes by a transitional period featured by the utilization of hybrid fossil/renewable integrated systems.

At present, large-scale and low-cost hydrogen production are essentially achieved by hydrocarbon reforming, mainly

Correspondence concerning this article should be addressed to A. Giaconia at alberto.giaconia@casaccia.enea.it.

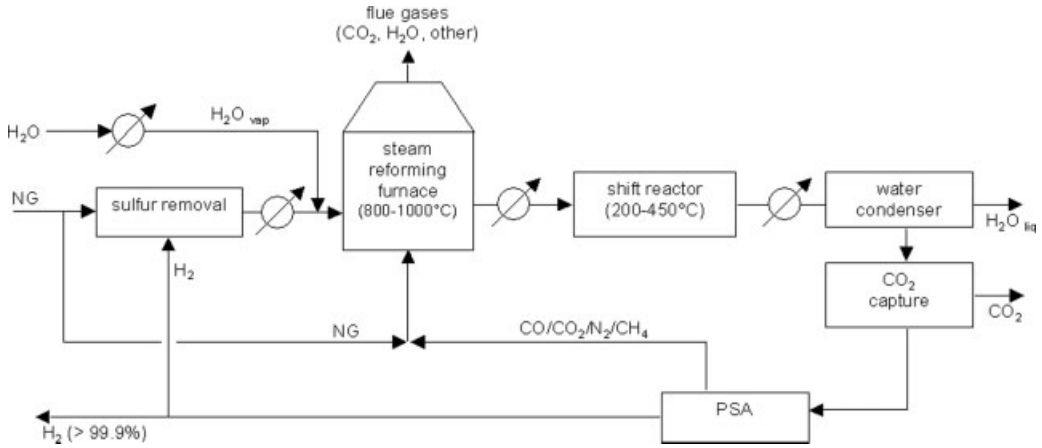

Figure 1. General sketch of a typical natural gas (NG) steam reforming process.

by steam methane reforming (SMR) basically consisting of two catalytic chemical reactions in the gas phase:

$$CH_4 + H_2O \rightarrow CO + 3H_2 \qquad (\Delta H_{298\,K} = +206\ \text{kJ/mol}) \tag{1}$$

$$CO + H_2O \rightarrow CO_2 + H_2 \qquad (\Delta H_{298\,K} = -41\ \text{kJ/mol}) \tag{2}$$

A simplified process sketch is shown in Figure 1.

Steam reforming reaction (1) of desulfurized natural gas is usually carried out at 800–1000°C in a furnace powered by crude natural gas. Differently, shift reaction (2) is exothermic and carried out at lower temperatures (200–450°C) to maximize the hydrogen yield, unless synthesis gas is the desired end-product (e.g. for methanol production). Hydrogen is purified afterward by pressure swing adsorption (PSA), while quantitative CO_2 capture can be achieved by adsorption in alkaline amine aqueous solutions.

Because natural gas (NG) represents both the reactant and the external power source (for steam generation, reforming furnace, purification, and auxiliary units), the real natural gas consumption strictly depends on the energetic efficiency of the process. For a large-scale plant with typical 70–85% energetic efficiency, methane consumption and the resulting CO_2 release are in the range of 3.0–3.7 kg_{CH4}/kg_{H2} and 8.3–10.1 kg_{CO2}/kg_{H2}, respectively. Differently, if an external non-fossil and carbon-free power source is used instead of natural gas to supply process heat, methane consumption, and CO_2 emissions will exclusively result from reaction stoichiometry, with specific values of 2.0 kg_{CH4}/kg_{H2} and 5.5 kg_{CO2}/kg_{H2}, respectively. Hence, a considerable reduction of greenhouse gas (GHG) release and fossil demand is achieved using an alternative external heat source.

Either nuclear or concentrating solar power (CSP) plants could be used as external carbon-free heat supplier. A number of scientific and technical papers related to these applications have appeared in the literature in the last years.[1–5] However, the management of large chemical plants coupled to nuclear or solar plants operating at temperatures up to 800°C still has a number of critical technological concerns dealing with materials resistance, costs, and safety. Moreover, very high temperature (>800°C) nuclear reactors (VHTR) are not yet commercially available, while coupling with the solar plants involves further chemical process control issues due to the power source irregularity.

Therefore, the exploitation of the above-mentioned technologies for GHG emission reduction and natural gas saving is feasible only if the reforming reactions are carried out at temperatures easily reachable with the currently available nuclear and solar technology, and if some plant management shortcomings related to discontinuous availability of the solar energy are overcome. In the case of solar-power plants, constant-rate heat supply is practicable by means of suitable heat storage systems and heat-transfer fluids to attenuate solar-radiation irregularities and protract chemical plant running overnight, eliminating daily start-up and shut-down operations.

Solar thermal technology has got great advancements in the last decades, especially for solar electric generating systems (SEGS).[6,7] Solar trough technology is now the most mature and checked technology, with 354 MW_{el} in operation in the southwestern United States (divided in nine different commercial-scale plants, the first built in 1984), where organic oils up to 350°C are largely used as heat-transfer fluids.[7] The use of thermal storage systems in SEGS has been proposed to eliminate the mismatch between energy supply by the sun and energy demand peaks.[8,9]

Recently, some molten nitrates mixtures demonstrated a viable large scale thermal storage medium, reaching storage efficiencies higher than 99% and the possibility to provide 24 h solar heat at constant rate[7] due to their high heat capacity per unit volume. Different from organic oils, molten nitrate mixtures are stable at high temperatures (up to 600°C), relatively inexpensive and widely available, not flammable, and have minor environmental impact; moreover, these molten salts have very low vapor pressure (i.e., do not require pressurized systems) and low corrosion rates with common-piping materials.[6,10,11]

One of the most promising molten salts for solar applications is the $NaNO_3/KNO_3$ (60/40 w/w) mixture, often referred as "solar salt," which has already been positively

long tested as solar heat carrier and heat storage medium up to 565°C in the Solar-Two pilot tower plant in Barstow (California) and will be used in the 15 MW_{el} Solar-Tres tower plant in Spain.[7,8,10]

Clearly, the utilization of such molten salts up to 550°C with a heat storage device can ensure constant-rate solar heat supply also for an energy demanding industrial chemical process like the SMR for hydrogen production. The continuous solar energy supply should enhance the process management avoiding daily start up and shut down operations despite the intermittent solar power availability. However, up to now, this technical possibility has not yet been thoroughly explored.

In this article, we propose a new solution to continuously power SMR by solar energy. Reforming reactions are carried out in tubular reactors and conversion enhanced by the use of membranes, and a mixture of molten salts at 550°C is used as storage means and thermal carrier of solar energy. The operating temperature lower than conventional allows to simultaneously drive the reforming and shift reactions (1 and 2) in the same reactor, but it is also a thermodynamic limit because of the endothermic nature of the reforming process; however, the use of hydrogen selective membranes allows equilibrium conditions to be not achieved and methane conversion to be improved. Different chemical process configurations have been developed and analyzed using a one-dimensional mathematical model to simulate the performance of the molten salt-heated reforming tubular reactors.

Process description

CSP plant. The concentrating solar power (CSP) plant basically consists of a solar collector field, a receiver, a heat-transfer fluid loop, and a heat-storage system. The mirrors of the solar field concentrate the direct solar radiation on the solar receiver set at the focal point. The heat-transfer fluid removes the high-temperature solar heat from the receiver, and it is afterward collected into an insulated heat storage tank to be pumped, on demand, to the heat users (steam generators, endothermic reactors, etc.) where it releases its sensible heat. Finally, the heat-carrier fluid is stored into a lower temperature tank to restart the solar heat collection loop during insolated hours.

In Figure 2, the CSP scheme is represented in the case of a solar trough system with molten salts heat carriers up to 550°C and two-tank molten salt storage, according to an innovative trough configuration conceived and developed by ENEA,[12] where molten nitrates $NaNO_3/KNO_3$ (60/40 w/w) are not only used as the storage medium, but are also the high temperature heat transfer fluid flowed in the receiver pipe. Receiver pipe (Figure 2a), designed as to resist at a maximum temperature of 580°C,[13] is located on the focal line of the linear parabolic mirrors and is composed of two concentric cylinders separated by a vacuum gap for thermal insulation: the external glass cylinder represents a protective casing, while the internal steel cylinder absorbs solar energy that is converted into high-temperature sensible heat of the molten salts. A spectrally selective coating compound for the receiver tube, developed and specifically designed by ENEA to maximize the efficiency at higher temperatures (550°C), covers the steel pipe and guarantees maximum absorption of solar radiation and reduction of infra-red emissions from hot tubes.[13]

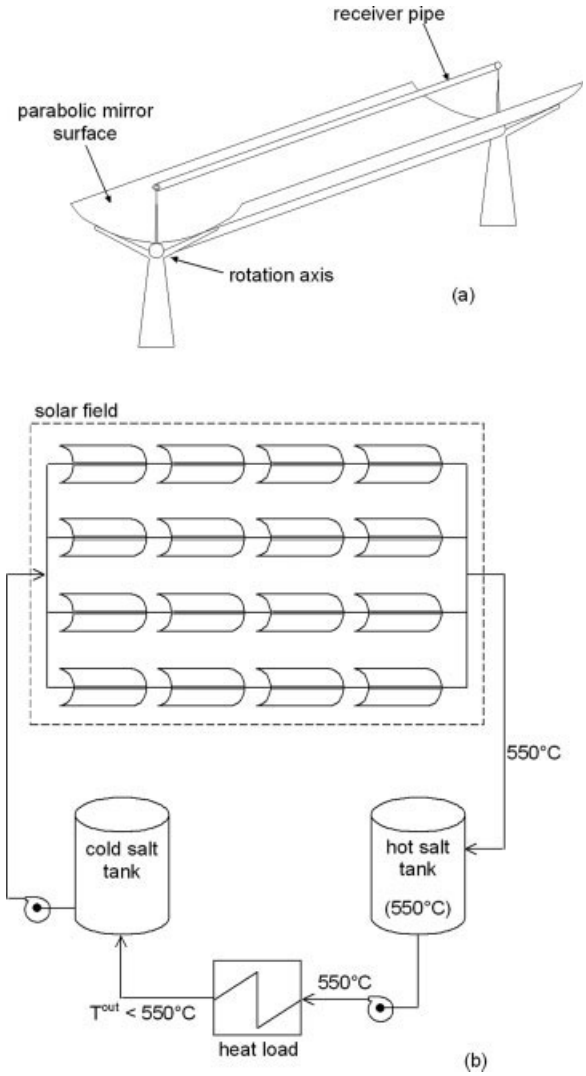

Figure 2. Simplified scheme of a single solar trough collector section (a) and a power plant with two-tank molten salt storage (b).

Two-tank (Figure 2b) or thermocline (i.e., single tank with temperature gradient along the height due to fluid stratification) systems can be applied for solar heat storage,[8,9] depending on the power plant size and storage capacity.

Such a solar collection system is easily adaptable to the features of a large number of potential sites in high-level solar radiation areas and can continuously provide thermal energy except for protracted cloudy periods (>3 days). Research finalized to further improvements is in progress for component cost reduction and material improvement.

This solar collection system is extensively and positively tested at the ENEA-Casaccia research centre using a 100-m long-linear parabolic trough test plant, while the construction of a 5 MW_{el} commercial plant is scheduled in the next years in Sicily for the "Archimede project" to integrate an already existing natural gas combined cycle power plant.

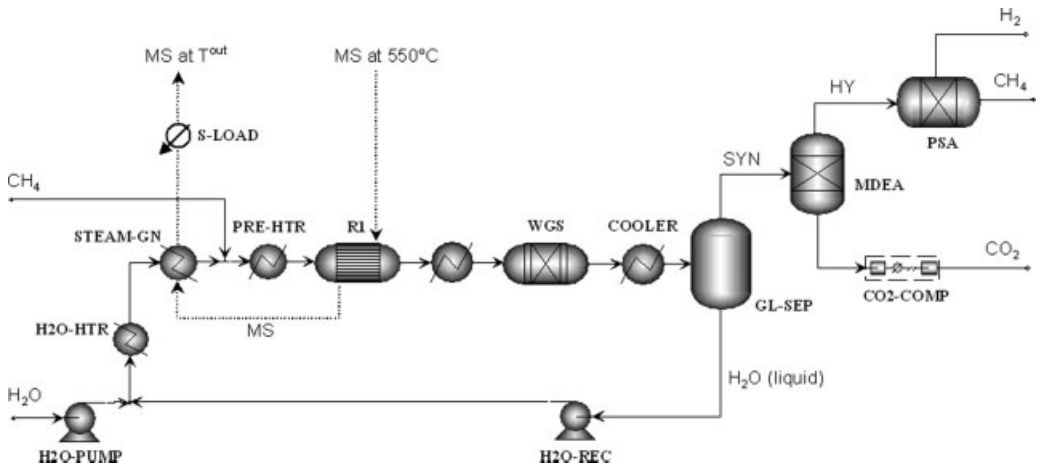

Figure 3. Flowsheet of SMR with single reactor.

Molten salts (MS) flow in dotted lines; S-LOAD: separation units duty (MDEA, PSA, etc.).

Steam Methane Reforming Plant. In Figure 3 the Basic SMR Plant Flowsheet is represented.

Different from conventional SMR plants (Figure 1), the basic reforming furnace is replaced by a more compact tubular heat exchanger reactor (R1), counter-currently flowed by the molten salts on the shell side. The inner tube packed with the catalyst is fed by the CH_4/H_2O gas mixture heated at about 500°C (in preheater PRE-HTR); molten salts from the hot storage tank of the solar plant (Figure 2b) have inlet temperature of about 550°C and cool down to lower temperatures (e.g. 530°C) by sensible heat transfer to the reacting mixture flowing in the inner tubes.

Under these conditions, reaction temperatures never exceed 550°C and methane conversion is limited. The product mixture (composed of $CH_4/H_2O/H_2/CO/CO_2$) is finally cooled down and purified. First, CO is removed by conversion to CO_2 in a water gas shift reactor (WGS) operating at lower temperatures (<450°C), and residual water is condensed and separated in a gas-liquid separator (GL-SEP). The gas phase is treated in a CO_2 capture unit (e.g., by adsorption in amine solutions, MDEA) and, finally, pure hydrogen can be optionally separated from nonreacted methane by PSA. Removed CO_2 can be liquefied (>100 bar) and sent to suitable stable disposal sites.

Molten salts exiting the reforming reactor (R1) at about 530°C are sent to the steam generator (STEAM-GN). Residual molten salts heat is also used to power other units such as the CO_2 removal and PSA units (S-LOAD). The resulting exit temperature of molten salt stream from the chemical plant (T^{out}) depends on the flow rate and is usually in the 450–510°C range: this will be the "cold" tank temperature of the CSP plant (Figure 2b), but considering that the minimum temperature of molten salts for practical management is around 290°C, further downstream services can be powered by the residual sensible heat of the fluid, such as electric power generation, heating, or water desalination.

If methane conversion on a single pass through SMR reactor (R1) is not satisfactory, different reaction stages in series can be applied (R1, R2, ...), with hydrogen removal by membranes (M1, M2, ...) set between catalyst beds: this way, a thermodynamic driving force due to hydrogen product removal enhances methane conversion to higher values despite the low temperatures. The flowsheet of a series of reactor and membrane modules is represented in Figure 4.

Methane conversion can be improved otherwise using a single tubular reactor (R1) with a partial recirculation of the product mixture after hydrogen removal in the permeator (M1). The general flowsheet of this configuration is represented in Figure 5.

Clearly, the use of suitable catalysts is recommended to carry out the SMR at lower temperatures than conventional and prevent irreversible coke deposition.[14,15]

Either dense metallic or porous ceramic membranes can be used to separate hydrogen from the SMR outlet gas mixture. Palladium-based dense membranes, with a permeability in the $10^{-7} - 10^{-8}$ mol/m/sec/$Pa^{1/2}$ range at operating temperatures at least up to 450°C,[16–20] allow a nearly pure hydrogen permeate flux (>99.99%) to be obtained. Porous ceramic membranes are less selective, but thermally and chemically more stable and, hence, more durable. Because membrane permeability and selectivity depend on working temperature, the temperature of the gas stream from SMR reactors may be adjusted to optimize the performances of the following membrane separator (Figures 4 and 5). In this work, Pd-based membranes are assumed to be used in the membrane modules and heat exchangers before the separators are needed to reduce the temperature down to the operating threshold imposed.

Because the driving force for permeation is the hydrogen partial pressure gradient across the membrane, a vacuum pump (H_2-COMP) has to be used to continuously extract the permeated hydrogen; in this case, the electrical consumption of this machine must be taken into account. Otherwise, superheated steam can be used as sweep gas: after expansion in a "low" pressure steam turbine and subsequent water condensation, hydrogen will be recovered, and electric power produced thereby. Although the latter method involves an additional steam cycle (possibly powered by the molten salts'

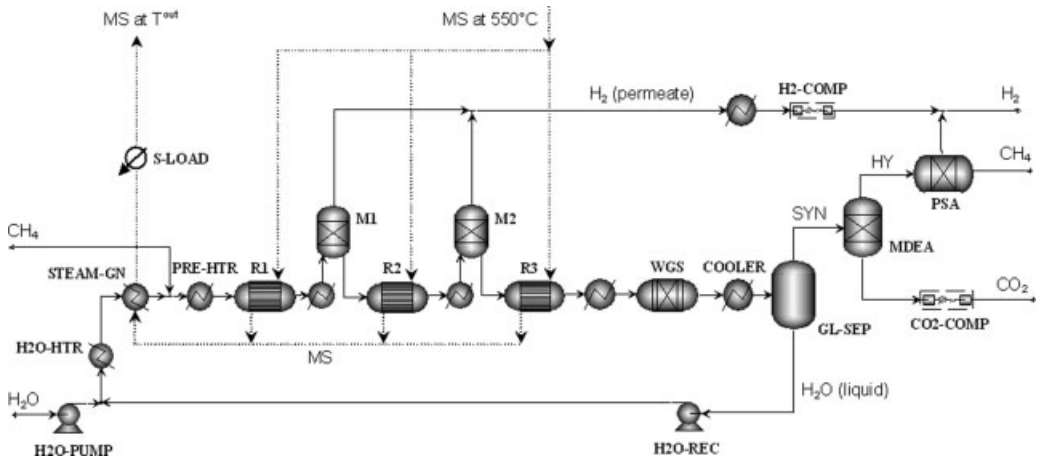

Figure 4. SMR configuration with three reactors (R1, R2, R3) in series and intermediate membrane units (M1, M2) for hydrogen removal.

Molten salts (MS) flow in dotted lines; S-LOAD: separation units duty (MDEA, PSA, etc.).

residual heat), it looks more reasonable in a cogenerative system where solar SMR is carried out along with solar electric power generation.

Process analysis

Molten salts assisted solar SMR has been analyzed by means of suitable mathematical models for catalytic steam reforming and water-gas-shift reactors, and the ASPEN Plus process simulator for flowsheet development with mass and energy balances. Data obtained from previous works[21] have been used for the properties of molten salts ($NaNO_3/KNO_3$, 60/40 w/w).

All chemical process configurations have been analyzed at nominal pressures of 10 and 20 bar, and 2.2 mol/mol steam-to-carbon ratio into first SMR reactor (R1).

SMR reactors have been modeled as double tube heat exchangers, with gas mixture entering the inner tube packed with catalyst bed at 500°C, and molten salts counter-current flowing in the annular zone entering at 550°C and with about 530°C exit temperature (Figure 6).

A one-dimensional mathematical model based on mass, energy, and momentum balances has been used to obtain composition, pressure, and temperature axial profiles in the reactors, both in gas and molten salt sides.

The reactions (1–2) and the global reaction:

$$CH_4 + 2H_2O \rightarrow CO_2 + 4H_2 \tag{3}$$

have been considered.

The model is based on the following assumptions:

(1) steady-state conditions;
(2) plug flow behavior;
(3) pseudohomogeneous catalyst bed;
(4) pseudoeffectiveness factors η_1, η_2, and η_3 for the reactions (1), (2) and (3) independent of local conditions and fixed at 0.02 as an average value of those reported in the literature[22–24];
(5) ideal gas behavior.

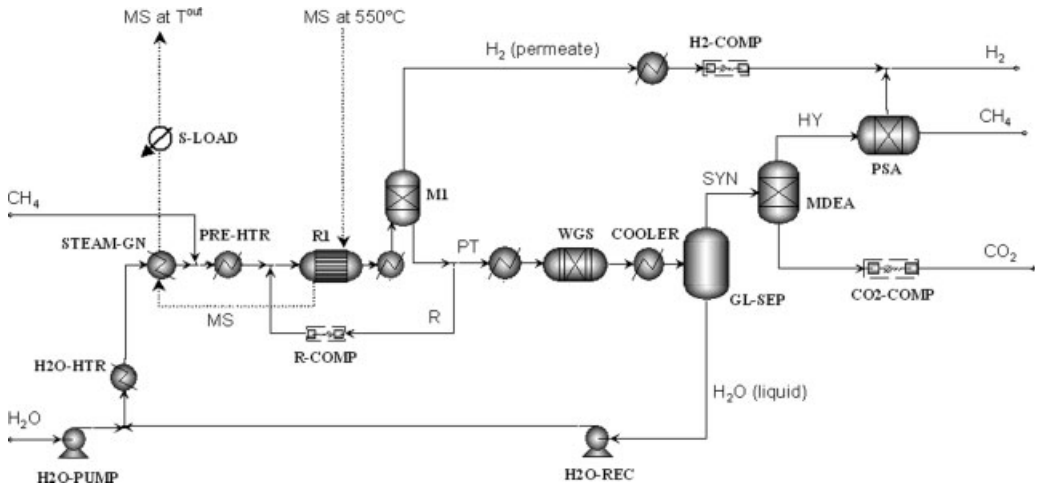

Figure 5. SMR configuration with a single reactor (R1) and partial recirculation product after hydrogen removal by membrane (M1).

Molten salts (MS) flow in dotted lines; S-LOAD: separation units duty (MDEA, PSA, etc.).

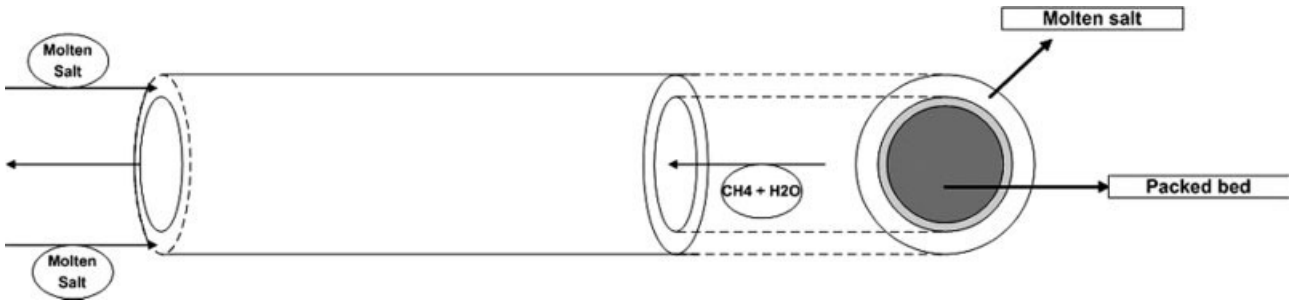

Figure 6. Draft section of the steam reforming reactor.

It has been demonstrated that the one-dimensional nature of the model does not lead to significant errors compared with a similar two-dimensional approach.[25] Therefore, the mathematical model can be considered a reliable tool for the assessment of the reformer behavior.[26]

The model is composed of the following ordinary differential equations:

- *Mass balances:*

$$\frac{dF_{CH4}}{dz} = -\rho_{app} \cdot (1-\varepsilon) \cdot \pi \cdot R^2 \cdot (\eta_1 \cdot r_1 + \eta_3 \cdot r_3)$$
$$\frac{dF_{H2O}}{dz} = -\rho_{app} \cdot (1-\varepsilon) \cdot \pi \cdot R^2 \cdot (\eta_1 \cdot r_1 + \eta_2 \cdot r_2 + 2 \cdot \eta_3 \cdot r_3)$$
$$\frac{dF_{CO}}{dz} = \rho_{app} \cdot (1-\varepsilon) \cdot \pi \cdot R^2 \cdot (\eta_1 \cdot r_1 - \eta_2 \cdot r_2)$$
$$\frac{dF_{CO2}}{dz} = \rho_{app} \cdot (1-\varepsilon) \cdot \pi \cdot R^2 \cdot (\eta_2 \cdot r_2 + \eta_3 \cdot r_3)$$
$$\frac{dF_{H2}}{dz} = \rho_{app} \cdot (1-\varepsilon) \cdot \pi \cdot R^2 \cdot (3 \cdot \eta_1 \cdot r_1 + \eta_2 \cdot r_2 + 4 \cdot \eta_3 \cdot r_3) \quad (4)$$

where F_i is the molar flow rate of the component i (i = CH_4, H_2O, H_2, CO, and CO_2), η_i are the effectiveness factors for the reactions considered, ρ_{app} and ε are the apparent density and the void fraction of the packed bed respectively, R is the reactor radius, and r_j is the rate of the reaction j (j = 1, 2, and 3), described by the Xu-Froment kinetic model.[27]

- *Energy balances:*

Reaction zone:

$$\left(\sum_{i=1}^{5} F_i \cdot c_{P,i}\right) \cdot \frac{dT}{dz} = U \cdot 2 \cdot \pi \cdot R \cdot (T_{MS} - T) + \rho_{app} \cdot \varepsilon \cdot \pi \cdot R^2 \cdot \sum_{j=1}^{3} \eta_i \cdot r_j \cdot \Delta H_j \quad (5)$$

Shell (molten salt zone):

$$w_{MS} \cdot c_{p,MS} \cdot \frac{dT_{MS}}{dz} = U \cdot 2 \cdot \pi \cdot R \cdot (T_{MS} - T) \quad (6)$$

where $c_{p,i}$ is the specific heat of the component i, ΔH_j is the reaction j enthalpy, w_{MS} and T_{MS} are the mass flow rate and the temperature of the molten salt stream.

U is the overall heat transfer coefficient between the shell and the reaction zone and takes into account a series of heat transport resistances:

1. the convective term in the molten salt zone;
2. the conduction of the tube wall;
3. the molecular conduction of the gas layer immediately near the tube wall[28];
4. the heat transport inside the packed bed, in which the assumption of pseudohomogeneous phase has been made, that is, the solid and the gas are considered as only one phase. The equation reported by De Wasch-Froment[29,30] has been used to evaluate this contribution.

- *Momentum balance* (only for the reaction zone):

$$\frac{dP}{dz} = -10^{-3} \cdot f_v \cdot G \cdot \frac{\mu}{\rho \cdot d_p^2} \frac{(1-\varepsilon)^2}{\varepsilon^3} \quad (7)$$

where G is the specific mass flow, μ and ρ are the viscosity and the density of the gas mixture, d_p is the catalyst particle diameter, and f_v is the friction factor, calculated by the well-known Ergun equation.

In all the equations of the model, the dependence of the gas mixture physical properties on temperature, pressure, and gas composition has been considered.

In Table 1, all the geometric features and physical properties for the steam-reforming reactors imposed in the simulations are reported. These data are the typical ones for an industrial steam-reforming reactor.

In the flowsheet analysis made with the ASPEN Plus simulator each reactor, either SMR and WGS reactors, has been modeled as a "stoichiometric reactor": fractional conversion (or molar extent) values of reactions were generated from application of the above-described mathematical model.

As far as the membrane modules are concerned, the use of Pd-based thin layer membranes supported on a ceramic or metallic material operating at 500°C is assumed; moreover, membranes are supposed sized so as to remove 85% of the inlet hydrogen with 100% selectivity. As constant temperature and pressure conditions have been assumed along the permeators, the adopted model only involves the mass balance across the membrane:

$$\frac{dF_{H2}}{dz} = -J_{H2} \cdot 2 \cdot \pi \cdot R \quad (8)$$

$$\frac{dF_{H2}^{perm}}{dz} = -J_{H2} \cdot 2 \cdot \pi \cdot R \quad (9)$$

where F_{H2}^{perm} is the hydrogen molar flow rate in the downstream. The sign "minus" in Eq. 9 means that a counter-current configuration has been imposed.

Table 1. Geometric Features and Physical Properties for the Steam Reforming Reactors Imposed in the Simulations

SMR Reactor Parameter	Value
Single reactor tube length (L)	12 m
Reactor inner radius (R)	0.065 m
Catalyst apparent density (ρ_{app})	1016.4 kg_{cat}/m^3
Catalyst particle diameter (d_p)	0.011 m
Packed bed void fraction (ε)	0.5
Effectiveness factors of reactions (η_j)	0.02

The term J_{H2} represents the hydrogen flux permeated through the membrane and it is calculated by the Sievert law:

$$J_{H2} = \frac{B_H}{\delta}\left(\sqrt{p_{H2}^{up}} - \sqrt{p_{H2}^{down}}\right) \quad (10)$$

where B_H is the Pd-based membrane permeability, δ is the membrane thickness, p_{H2}^{up} and p_{H2}^{down} are the hydrogen partial pressure up and downstream. Typical Pd-based membrane technology values of $\delta = 20$ μm and $B_H = 2.754 \times 10^{-6}$ kmol/(m h $kPa^{0.5}$) have been assumed in this study.[31]

The permeated hydrogen is extracted by means of an extractor fan (H_2-COMP). Therefore, the Pd-based membrane should be suitably supported in such a way to resist to the pressure stresses (up to 10 or 20 bar of difference across the membrane).

This model has been used to size the membrane to attain the specified hydrogen removal (85% of feed content) and to determine the power duty of the hydrogen extraction system. In the ASPEN Plus simulations, membrane modules (M1, M2, etc.) have been modeled as isothermal component separators with hydrogen split fraction of 0.85, and hydrogen permeate extraction pump (block H_2-COMP) modeled as a 3-stages isentropic multistage compressor.

As regards the downstream purification units, the produced CO_2 is completely separated from the SYN mixture (Figures 3–5) by adsorption in amine solutions in the MDEA unit. Similarly to membrane modules, in the ASPEN Plus simulations simple component separator blocks have been applied for the MDEA and PSA units, assuming 1.00 as CO_2 and hydrogen split fraction.

The amine solution of MDEA is regenerated, and the extracted CO_2 is liquefied at 100 bar and room temperature to enhance subsequent disposal. The thermal and electric duties of the CO_2 capture and liquefaction unit (MDEA + CO_2-COMP) have been assumed to be 2.32 GJ_{th}/ton_{CO2} and 63.1 kWh_{el}/ton_{CO2},[32] with the thermal duty supplied by the molten salts' residual sensible heat (S-LOAD unit). Differently, the PSA unit consumption has been neglected.

Finally, as far as the remaining flowsheet blocks are concerned, recirculation compressor R-COMP (Figure 5) has been modeled as isentropic single-stage compressor. Heat released by gas coolers following SMR reactors and the heat from the WGS reactor is recovered in heater H_2O-HTR, whereas the heat from the final cooler (block COOLER) is wasted.

Results and Discussion

Assuming 3 kmol/h as methane feed flow rate, in the case of a single reactor (Figure 3), methane conversion of 16–21% has been obtained, resulting into the production of enriched methane, i.e., a H_2/CH_4 mixture (HY). Correspondingly, CO_2 capture leads to 16–21% of natural gas decarbonization: this is the reduction rate of CO_2 emissions of the gas final user. Because the heat value of this outlet mixture is higher than the pure methane feedstock a feed heat value upgrading of 4.5–5.8% is achieved by this way. This value represents the solar energy captured and stored in the form of hydrogen energy.

Molten salts exit temperature (T^{out}) from the chemical plant (including CO_2 capture unit) is about 470 or 460°C, in the scheme operating at 10 or 20 bar, respectively. Afterward, molten salts can be stored in the "cold" heat storage tank (Figure 2), to be recirculated in the solar collection plant during the insolation hours; otherwise, molten salts can be further cooled to supply other plants requiring lower temperature heat duty (e.g., steam generation). The electrical consumption is about 2–3 kW (for 3 kmol/h of methane feed rate), almost entirely due to the CO_2 capture/liquefaction unit (MDEA + CO_2-COMP).

The introduction of hydrogen permselective modules between SMR reactors (Figure 4) enhances methane conversion and the simultaneous production of a hydrogen-rich (permeate) stream besides the enriched methane (HY). The total molten salts flow rate from the hot tank is split between SMR reactors (R1, R2, etc.) connected in parallel with respect to the molten salts (Figure 4): inlet temperature of molten salts in each reactor is 550°C, with flow rate depending on reactor thermal load.

As plotted in Figure 7, methane conversion and feed heat value upgrading (HHV basis) increase by increasing the number of reaction stages in series: methane conversions of 54–69% (and an equivalent decarbonization rate) can be obtained in the case of six reaction stages, while the produced enriched methane stream (HY) still has a high hydrogen content, being in the range of 39–56% vol. Moreover, feed heat value upgrading can be raised from about 5 to 20% by increasing the reaction stages and reducing the operative pressure.

The larger the number of reaction stages, the larger are methane conversion and the required molten salts flow rate, and the higher the temperature (T^{out}) of the molten salts exiting the chemical plant, being as high as 508°C in the configuration with six reactors at 10 bar nominal pressure. Moreover, when membranes are used the electric duty of hydrogen extraction multistage compressor H_2-COMP must be accounted in the energy balance: this additional electric consumption depends on membrane active surface and can be optimized for cost reduction, as discussed in the following section.

It is noteworthy that the reactor/membrane units train is fairly equivalent to a single membrane-integrated reactor, that is, a reactor equipped with the membrane tube set inside the catalytic bed: the use of membranes working at temperatures close to SMR reactor temperatures (530°C–550°C) should allow us to design compact membrane reformers powered by molten salts at 550°C, with resulting axial conver-

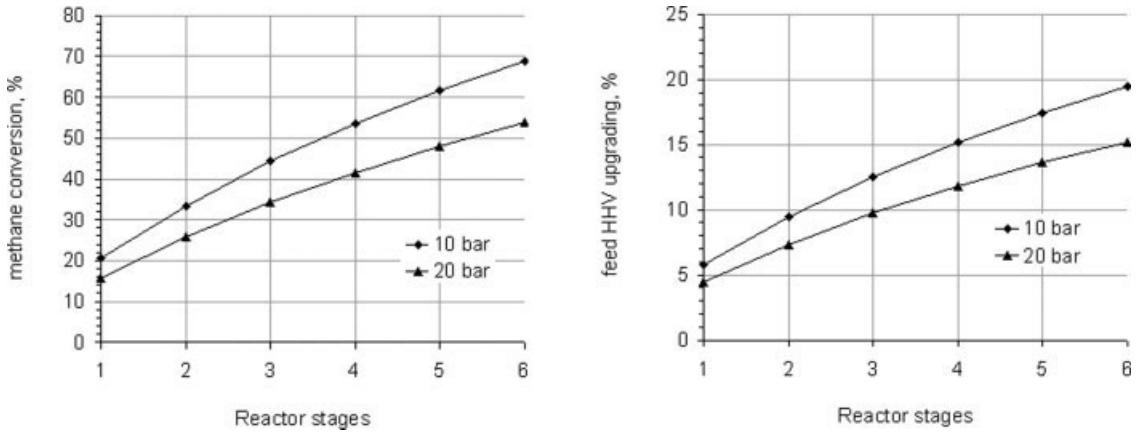

Figure 7. Methane conversion and heat value upgrading vs. number of SMR reaction stages.

sion profiles fairly equivalent to those plotted in Figure 7. The design of such a single unit is an important chemical engineering challenge dealing with the matching of the three main driving process mechanisms: heat transfer from the heating fluid to reacting gas, reaction catalysis and kinetics, and hydrogen permeation rate through the membrane.[20,33–35] On the other hand, separation of reaction from permeation zones (e.g., by multi-stage arrangements) enables us to run each unit at the optimum operative conditions and may ease maintenance operations.

Methane conversion by the use of membranes can be alternatively enhanced using a single reactor followed by a membrane module and with partial recirculation of the gas after hydrogen removal (Figure 5). In this case, we can define the reflux ratio R as the ratio between recirculated (F_R) and non-recirculated (F_{PT}) flow rates:

$$R = \frac{F_R}{F_{PT}}$$

The performance of this process configuration is plotted in Figure 8 with R ranging from 0 to 2. Obviously, the results approach those obtained with a single reactor without membrane separation when R comes down to zero.

Methane conversions (and decarbonization rates) are the order of 21–32%, with 6–9% feed heat value upgrading. Both values increase with the reflux ratio; higher reflux ratio can be reached at higher working pressure. The produced enriched methane stream (HY) has always a hydrogen content in the range of 12–19% vol. Molten salt exit temperature (T^{out}) is within the range of 465–482°C in this case.

Partial recirculation of product mixture (after 85% hydrogen removal) causes a higher CO_2 concentration in the reactor, which results in a lower hydrogen partial pressure in the reactor outlet mixture, until hydrogen permeation becomes not practical at higher reflux ratios and lower pressures (e.g., at 10 bar and $R = 2.0$).

Again, the appropriate design of a single molten salt-heated membrane reactor with internal partial recirculation of the gas mixture exiting the catalyst bed can be an interesting tool to improve the process in terms of compactness, performance, and costs.

In Figure 9, the solar plant size per unit hydrogen produced is reported for all the process configurations here considered. This is an important parameter as the CSP plant is a major investment cost item for the process. The addition of membranes permits to drastically reduce the CSP plant size, especially when two or three reactor/permeator units in series are used in place of a single reactor (Figure 9a). A consider-

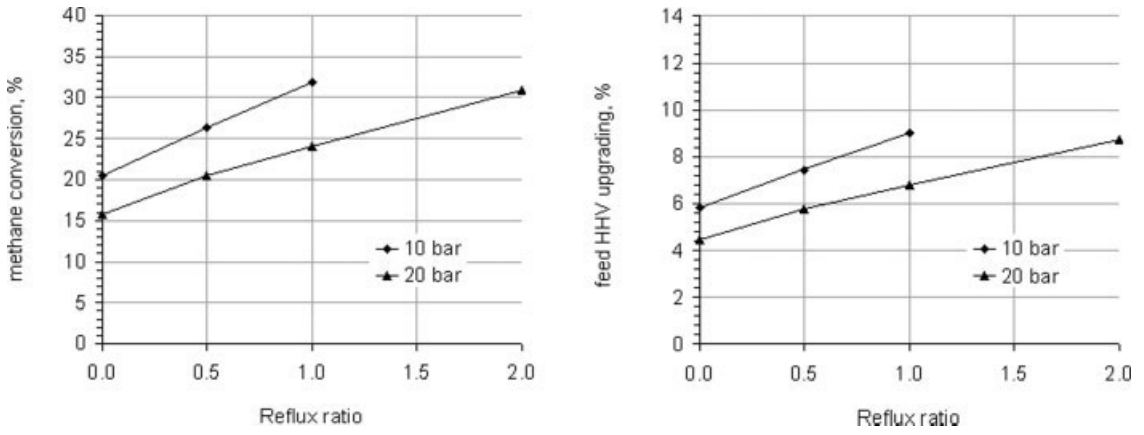

Figure 8. Methane conversion and heat value upgrading vs. reflux ratio.

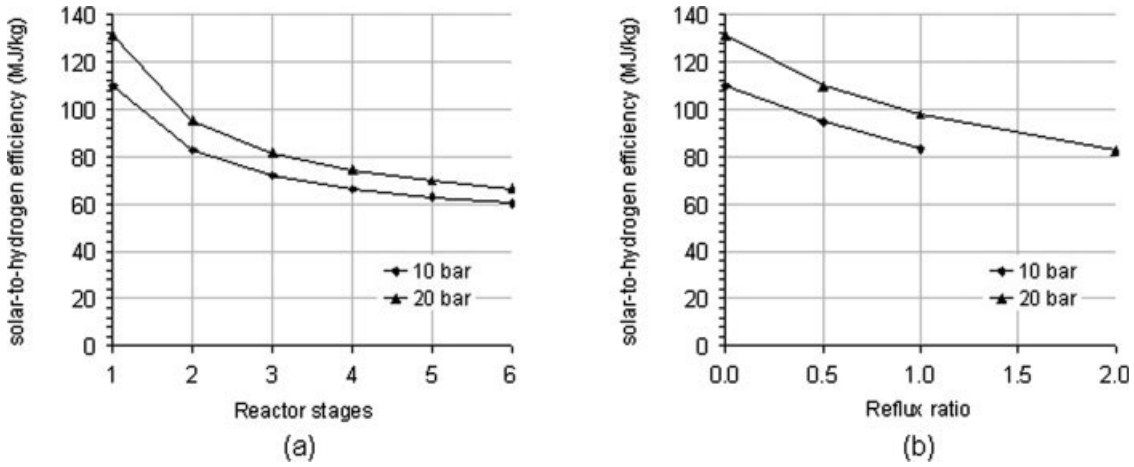

Figure 9. Heat required from solar plant per unit hydrogen production for the process configurations presented: 1 to 6 reactors in series (a), single reactor with reflux (b).

able reduction of the solar heat demand by the use of membranes is also obtained in the scheme with single reactor and partial reflux (Figure 9b). This behavior is essentially due to the higher methane conversion that results in a lower water recirculation rate to be revaporized in STEAM-GN units.

To assess the potentialities and competitiveness of the conceived conversion process, basic figures of merit to be evaluated are production costs, net CO_2 emissions reduction, natural gas consumption, and land utilization.[36] Additionally, the potential spin-off in chemical and energy industry enhanced by solar-powered hydrogen production and natural gas enrichment should be considered.

Sizing and costing

From the economical standpoint, molten salt-assisted solar SMR combines the most actually used and low-cost industrial hydrogen production route (i.e., steam reforming of natural gas), with the very efficient, promising and nearly mature CSP technology of solar heat storage.[6,7]

Clearly, suitable criteria must be adopted for both chemical and solar power plant sizing and their coupling to optimize costs and to enhance practical process management.

As far as the chemical plant is regarded, the extraction device of permeated hydrogen from membrane modules must be identified. In Figure 10, the relationships between hydrogen pressure in the permeate p_{H2} and membrane active surface A_m are plotted for each membrane of the chemical plant configurations studied. We assumed that hydrogen is extracted by a fan and that mechanical properties of supported membranes enable to operate with pressure differences of 10 or 20 bar; hence, assuming the hydrogen permeated pressure p_{H2} and total feed mixture pressure p_{FM} both constant along the membrane module axis, according with the Sievert equation for dense membranes (Eq. 10), we get:

$$dA_m = \frac{\delta}{B_H} \cdot \frac{dF_{H2}}{\sqrt{\frac{F_{H2}}{F_{H2}+F_I} \cdot p_{FM}} - \sqrt{p_{H2}}} \tag{11}$$

where δ and B_H are membrane active thickness and permeability, respectively, and F_I is the flow rate of nonpermeating components in the feed (CH_4, H_2O, CO, and CO_2).

Suitable values of $\delta = 20$ μm and $B_H = 2.754 \times 10^{-6}$ kmol/(m h $kPa^{0.5}$), and 85% extraction ratio has been assumed in Figure 10.

Obviously, the driving force for permeation is reduced by increasing the hydrogen pressure in the permeate p_{H2}, and a maximum limit value is obtained when p_{H2} equals the hydrogen partial pressure in the feed mixture (driving force sets to zero under this condition). Because the higher the p_{H2} the lower is the electric duty for the extraction machine H_2-COMP and the higher the membrane cost, a suitable compromise value of p_{H2} should be adopted to minimize costs, as illustrated in Figure 11.

Similar considerations are pertinent when sweep steam is used to extract hydrogen, except for the electrical duty of the H_2-COMP that is replaced by a steam generation duty (that can be powered by the solar salts too); in this case, the steam-rich permeate total pressure can approach the pressure on the feed side and, hence, the mechanical resistance of the membrane is of minor concern.

The possibility to use much less costly ceramic membranes in place of the dense Pd-based ones, and/or the use of integrated membrane reactors, as previously discussed, can be considered in the technical-economic evaluation if a very high degree of pureness of the hydrogen is not required (microporous ceramic membranes are less selective than dense metallic ones).

Additional room available for economic optimization deals with the coupling of the chemical plant with the CSP plant. The chemical plant basically consists of compact tubular reactors and membrane modules and may be composed of modular parallel units to "follow" the seasonal solar energy availability. As a matter of fact, for a given solar field area and heat-storage capacity, a larger molten salts flow rate is available in the sunnier seasons, when "full load" operation of the chemical plant is feasible; differently, in the periods with lower average solar radiation a "partial load" of the chemical plant is possible by closing some process lines.

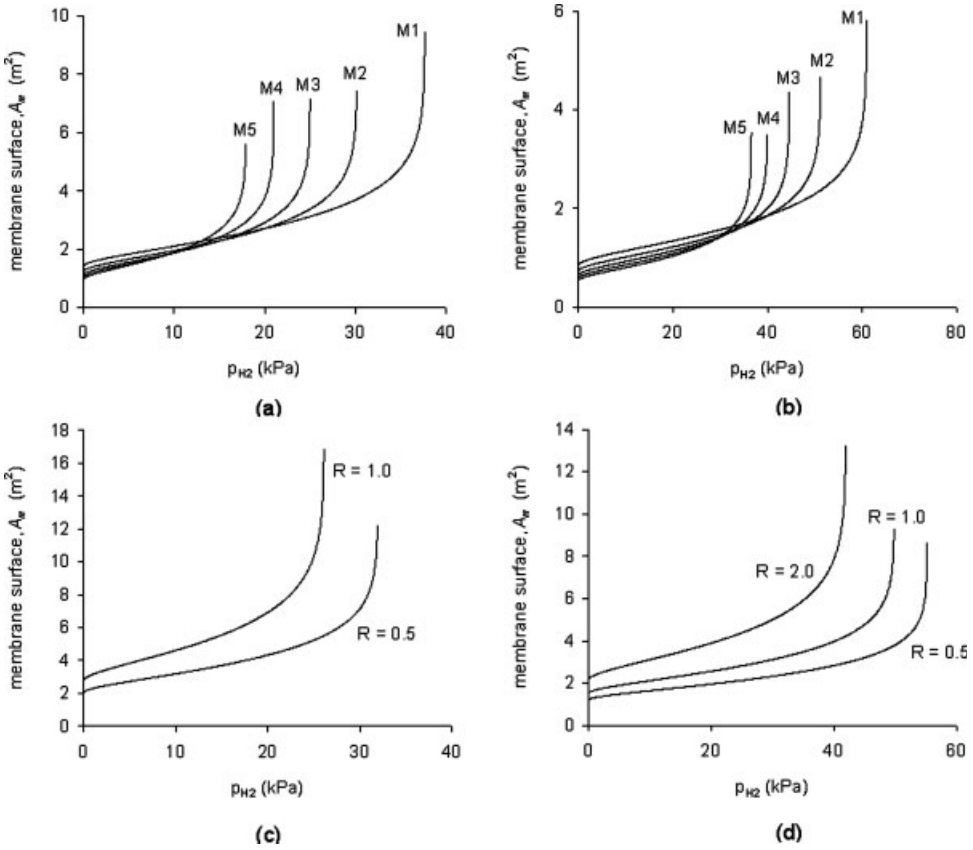

Figure 10. Relationships between hydrogen pressure in the permeate p_{H2} vs. membrane active surface A_m in the chemical plant schemes studied.

SMR reactors/permeators in series at 10 bar (a) and 20 bar (b), and SMR single reactor/permeator with partial recycle at 10 bar (c) and 20 bar (d). H_2 extraction ratio = 85%; membrane active thickness = δ = 20 μm; membrane permeability = $B_H = 2.754 \times 10^{-6}$ kmol/(m h kPa$^{0.5}$).

This strategy leads to the optimal utilization of the available solar power and, then, to the best exploitation of the solar plant that is one of the highest fixed cost items. Another option is the utilization of a fossil-powered back-up to heat up the molten salts (to 550°C) when solar energy is not adequate to satisfy the chemical plant heat demand.

Moreover, it is clear from Figure 9 that membrane application will reduce the size (and cost) of the CSP plant but, on the other hand, certainly increases the cost for the chemical process: again, the best compromise between membrane exploitation and solar plant size (land utilization) must be determined.

Therefore, a precise and reliable estimation of the lower bound hydrogen production cost results from an accurate process design and optimization study, by considering all the above-mentioned options (SMR process configuration, steam-to-carbon feed ratio, permeate hydrogen extraction system, membrane type, solar-to-chemical plant matching, CO_2 capture system, molten salts residual heat recovery in other plant units, thermocline or two-tank solar thermal storage system, etc.) and other basic assumptions (insolation of the reference site, plant life, annual working hours, taxation, incentives, natural gas and electricity unit costs, etc.).

Nevertheless, an approximate evaluation of the hydrogen production cost (HPC) has been done considering a nominal hydrogen production of 20,000 Nm^3/hour for 300 days of continuous running (e.g., from 20 January to 15 November).

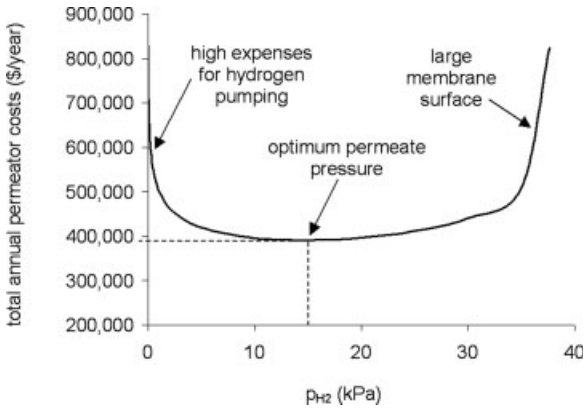

Figure 11. Example of relationship between annual costs for the hydrogen membrane separation system and hydrogen permeate pressure p_{H2}.

Nominal hydrogen output = 5000 Nm^3/h; membrane cost = 5600 \$/m^2; electricity cost = 6.5 c\$/kWh.

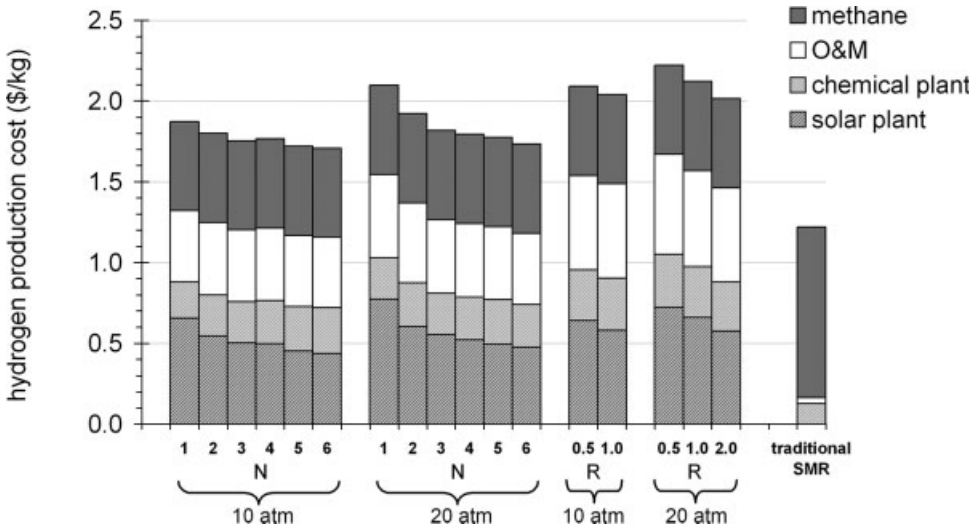

Figure 12. Hydrogen production cost (HPC) estimation for the different molten salt assisted solar SMR configuration studied and comparison with the traditional SMR process.

Membrane separators have been optimized as aforesaid (Figure 11), considering Pd-based membranes (costing 5,600 $\$/m^2$) and the hydrogen permeate extracted by a fan.

The best solar-to-chemical plant matching has been studied with a series of simulations. The solar plant is assumed to have optical efficiency of 0.8; differently, the solar plant thermal efficiency varies with the instantaneous irradiation and has been computed by a thermal simulation. A 5% loss due to piping has also been considered. The hour irradiation sequence measured at Priolo Gargallo near Siracuse in Sicily (Italy) in the year 2003 has been used as input data. At each hour, the overall solar-to-thermal efficiency (= optical * thermal efficiency) of the solar plant and the resulting delivered thermal power are computed. The main design parameters to optimize are the effective area of the solar field A and the energy storage capacity C: hence, for each of the 17 configurations, the optimal values of A and C to minimize the HPC have been obtained.

The cost of the solar field is estimated at 260 $\$/m^2$, including land, yard improvement, installation, mirrors, receivers, piping, and service facilities. The cost of the heat-storage system comprises the tank cost, roughly proportional to the tank wall area (assumed 1170 $\$/m^2$), and the cost of the salt (0.75 \$/kg), whose required amount is proportional to the storage capacity C.

The following annual operation and maintenance (O&M) costs have been considered:

- operative costs (personnel, insurance, etc.) for both chemical and solar plants assumed to be 2% of fixed capital investment;
- the cost for the periodical maintenance of the membranes assumed to be, yearly, the 20% of the purchased membrane cost (5600 $\$/m^2$);
- the cost of the electricity (0.065 \$/kWh), methane (0.26 $\$/m^3$), and water (0.001 \$/kg) consumed.

The annual costs have been actualized assuming a discount rate of 5%, and an inflation rate of 2%, for a plant life of 20 years.

The results are shown in Figure 12, where also the costs of a conventional process (under the same economic assumptions) are reported for comparison. In the scheme with a single reactor without the use of membranes (Figure 3), the major cost voice of chemical plant is the steam generator, being around 50% of the total purchased chemical plant equipment. Differently, when membranes are used, the membrane units with the hydrogen extraction system are the major investment cost item of the chemical plant (ranging from about 30 to 50%), followed by other separation units (MDEA and PSA, about 30%) and steam generator. The trend reported in Figure 12 shows that HPC can be reduced by membrane exploitation in multistage reactor/membrane arrangements (Figure 4) and/or increasing the reflux ratio R in the scheme with partial recycle of the nonpermeated stream (Figure 5). Considerable plant and operative cost reduction can be achieved using less costly membranes, because the Pd membrane cost (5600 $\$/m^2$) here assumed can be considered an upper value; moreover, the income from valuable Pd recovery at the end of plant life was not considered in this analysis.

However, the HPC values of 1.7–2.2 \$/kg here obtained are in agreement with those elsewhere reported for SMR powered by external alternative sources, either nuclear (at 550°C with membranes) or solar (central receiver reactor at 900°C).[4,37]

The resulting capital costs of the solar salts powered SMR are higher than conventional SMR (ca. 1.2 \$/kg, Figure 12) because of the more complex chemical plant with membranes, the additional CSP plant, and the higher O&M costs. On the other hand, the natural gas cost incidence on the HPC for the solar SMR is within the range of 25–32%, much lower than the conventional process where the HPC is about 87% affected by the natural gas price (Figure 12). Therefore, a cost break-even point is predicted in the future,[4] with the solar route becoming more competitive as soon as plant costs decrease (both solar and chemical), natural gas price increases, and the CO_2 emissions reduction is supported (e.g., by "green certificates").

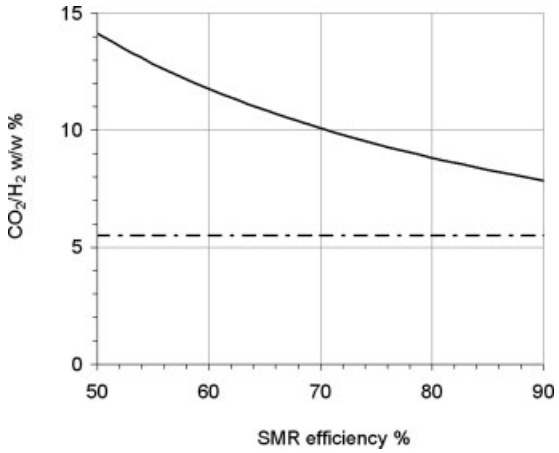

Figure 13. Comparison between conventional (solid line) and solar (dotted line) SMR in terms of specific CO_2 emissions related to overall process thermal efficiency (HHV basis).

CO_2 emissions reduction and natural gas saving

Whereas CO_2 emissions in conventional SMR strictly depend on the reforming furnace efficiency, solar SMR only uses renewable (CO_2-free) process heat, and the resulting specific CO_2 emissions will be about 5.5 kg_{CO2}/kg_{H2} (including also the water-gas-shift reaction), regardless the overall thermochemical process efficiency. In Figure 13, the two processes are compared: because common industrial processes have thermal efficiencies the order of 60–85%, a reduction of CO_2 emissions between 34 and 53% can be obtained by integration with the CSP plant. CO_2 reduction rate is more considerable at the smaller plant scales.

Moreover, it is noteworthy that the use of membranes for hydrogen removal enhances the CO_2 capture unit. As a matter of fact, because a large amount of the produced hydrogen is removed upstream, a higher CO_2 concentration in the final mixture (SYN) is obtained and, hence, CO_2 capture becomes more favorable and size and costs of the CO_2 separation unit (MDEA in Figures 3–5) will be reduced.

Natural gas savings, which clearly mean a CO_2 reduction rate (i.e., 34–53%), result in a minor implication of fossil supplying concerns.

Potential spin-off in the chemical and energy industry

As already discussed, the process here described involves compact reforming reactors and a solar trough plant that, differently from the solar tower system, can be modulated.[7] This results in a high scale-down potential leading to the development of small-medium scale installations where limited flow rates of pure hydrogen are demanded, with an estimated minimum hydrogen production rate being the order of 200–1000 kg/day.

For example, partial solar conversion of natural gas to hydrogen can enhance the "in situ" desulphurization of crude natural gas itself when the extraction well is sited on a satisfactorily insolated region. The continuous increase of natural gas price may lead to extraction from wells not yet used because of the high sulfur content of the crude gas (as it is for some reservoirs in South Italy), and "solar desulphurization" a way to increase the sustainability of the process.

The enriched methane produced by the molten salt assisted solar SMR is also a very valuable energetic product that can nowadays find several applications.[38–40]

First, it can be injected in the natural gas (NG) grid.[38,39] As a matter of fact, the current NG grid and final use tools are also suitable for NG/hydrogen mixtures within a concentration limit, commercially known as Hythane®. Hence, solar SMR can be a feasible and ready-to-use route for solar energy storage and transmission through the actual infrastructure, with a partial fossil decarbonation achieved thereby. This process can be interestingly set close to extraction wells or NG regasification plants; in this latter case, the residual molten salt heat may also power the gasification process itself.

Second, produced NG/hydrogen blends, within a concentration range, can be used in existing internal combustion engines (ICE), leading to a significant reduction of local pollution, especially in congested urban environments.[39]

Finally, solar-fossil hybrid options have been proposed by the integration of a highly efficient natural gas Combined Cycle Power plant (CCP) (using a NG gas turbine) with a CSP plant[7]: in this Integrated Solar Combined Cycle System (ISCCS), the steam from the solar steam generator integrates the steam Rankine cycle, increasing the steam turbine power. Differently, by using molten salts at 550°C from the CSP plant, the NG fed to the CCP can be pretreated and converted to enriched NG before entering the gas-turbine cycle[40]: hence, solar heat does not only power the Rankine steam cycle, but can also upgrade the value of the primary fuel in the high efficient gas-turbine cycle. Furthermore, efficiency improvements in the electricity generation can be achieved by means of fuel cell systems powered by the pure hydrogen produced thereby.

Summary and Conclusions

Recent advancements in solar-thermal technology have demonstrated the great potentials of the use of the molten nitrate mixture $NaNO_3/KNO_3$ (60/40 w/w) as solar heat carrier and storage medium at temperatures up to 565°C. On one hand, this high temperature storage concept enhances key benefits in solar-electricity generation; on the other hand, it enables us to drive highly energy demanding chemical processes like the methane steam reforming for hydrogen production, as it is presented in this article.

The use of solar energy as external process heat source in methane steam reforming allows at least 34% fossil fuel saving and, hence, an equivalent CO_2 release reduction.

Different chemical process schemes have been studied using a one-dimensional mathematical model for both the molten salt heated SMR and WGS tubular reactors; the AspenPlus process simulator was used for flowsheet development and analysis.

Results demonstrate that the application of hydrogen permselective membranes allows us to sensibly increase single-pass methane conversion and heat value upgrading, either in multistage arrangements or by the use of a single SMR reactor with partial recycle of the nonpermeated stream. Additional outstanding positive features deriving from the use of

membranes are the reduction of the CSP plant (size and costs) since the solar-to-hydrogen energy conversion efficiency is maximized, while the costs for CO_2 capture are reduced. The lower incidence of natural gas price on the hydrogen production cost will make this process competitive with the traditional route in the future as the natural gas price increases.

Several process configurations and operating conditions must be considered for plant design and technical-economical optimization. Because of the great scale-down potential and the possibility to produce pure hydrogen and/or enriched natural gas, some interesting applications and impacts in the current energy and chemical industry context have been discussed.

To conclude, this process involving the combination of different innovative and emerging technologies like CSP systems, molten salts heat transfer fluids, membranes, and "low" temperature methane reforming can be a response to the environmental concerns related with fossil decarbonization and solar energy conversion to chemical fuels.

Acknowledgments

The authors are grateful to KTI-Technip S.p.a. for useful information about plant cost estimation.

Literature Cited

1. Bohmer M, Langnickel U, Sanchez M. Solar steam reforming of methane. *Sol Energy Mater*. 1991;24:441–448.
2. Tamme R, Bruck R, Epstein M, Fisher U, Sugarmen C. Solar upgrading of fuels for generation of electricity. *ASME J Sol Energy Eng*. 2001;123:160–163.
3. Kodama T. High-temperature solar chemistry for converting solar heat to chemical fuels. *Prog Energy Combust Sci*. 2003;29:567–597.
4. Möller S, Kaucic D, Sattler C. Hydrogen production by solar reforming of natural gas: a comparison study of two possible process configurations. *ASME J Sol Energy Eng*. 2006;128:16–23.
5. Petrasch J, Steinfeld A. Dynamics of a solar thermochemical reactor for steam-reforming of methane. *Chem Eng Sci*. 2007;62:4214–5228.
6. Mills D. Advances in solar thermal electricity technology. *Sol Energy*. 2004;76:19–31.
7. Sargent & Lundy LLC Consulting Group. Assessment of parabolic trough and power tower solar technology cost and performance forecasts. NREL Subcontractor Report, NREL/SR-550-34440, October 2003.
8. Herrmann U, Kelly B, Price H. Two-tank molten salt storage for parabolic trough solar power plants. *Energy*. 2004;29:883–893.
9. Pacheco JE, Showalter SK, Kolb WJ. Development of a molten-salt thermocline thermal storage system for parabolic trough plants. *ASME J Sol Energy Eng*. 2002;124:153–159.
10. Herrmann U, Kearney DW. Survey of thermal energy storage for parabolic trough plants. *ASME J Sol Energy Eng*. 2002;124:145–151.
11. Kearney D, Herrmann U, Nava P, Kelly B, Mahoney R, Pacheco J, Cable R, Potrovitza N, Blake D, Price H. Assessment of a molten salt heat transfer fluid in a parabolic trough solar field. *ASME J Sol Energy Eng*. 2003;125:170–176.
12. The ENEA Working Group. Solar thermal energy production: guidelines and future programmes of ENEA. ENEA Report, ENEA/TM/PRESS/2001-07, June 2001.
13. Rubbia C, Antonaia A, Esposito S. Surface coating of the receiver tube of a linear parabolic solar collector. EP 1397622 (2004).
14. Matsumura Y, Nakamori T. Steam reforming of methane over nickel catalysts at low reaction temperature. *Appl Catal*. 2004;258:107–114.
15. Kusakabe K, Sotowa K-I, Eda T, Iwamoto Y. Methane steam reforming over Ce-ZrO_2-supported noble metal catalysts at low temperature. *Fuel Proc Technol*. 2004;86:319–326.
16. Barbieri G, Di Maio F. Simulation of the steam reforming process in a catalytic Pd-membrane reactor. *Ind Eng Chem Res*. 1997;36:2121–2127.
17. Gallucci F, Paturzo L, Basile A. A simulation study of steam reforming of methane in a dense tubular membrane reactor. *Int J Hydrogen Energy*. 2004;29:611–617.
18. Kim J, Choi B, Yi J. Modified simulation of methane steam reforming in Pd-membrane packed bed type reactor. *J Chem Eng Japan*. 1999;32:760–769.
19. Marigliano G, Barbieri G, Drioli E. Effect of energy transport on a palladium-based membrane reactor for methane steam reforming process. *Catal Today*. 2001;67:85–99.
20. Feng W, Tan T, Ji P, Zheng D. Exploration of hydrogen production in a membrane reformer. *AIChE J*. 2006;52:2260–2270.
21. Bradshaw RW, Carling RW.A review of the chemical and physical properties of molten alkali nitrate salts and their effect on materials used for solar central receivers. Sandia National Laboratiries Report, SAND87–8005, April 1987.
22. Rostrup-Nielsen JR. Production of synthesis gas. *Catal Today*. 1993;18:305–324.
23. Xu J, Froment G. Methane steam reforming II: diffusional limitations and reactor simulation. *AIChE J*. 1989;35:97–103.
24. Pedernera MN, Piña J, Borio DO, Bucalà V. Use of a heterogenous two-dimensional model to improve the primary steam reformer performance. *Chem Eng J*. 2003;94:29–40.
25. De Falco M, Di Paola L, Marrelli L, Nardella P. Simulation of large-scale membrane reformers by a two-dimensional model. *Chem Eng J*. 2007;128:115–125.
26. De Falco M, Di Paola L, Marrelli L. Heat transfer and hydrogen permeability in modeling industrial membrane reactors for methane steam reforming. *Int J Hydrogen Energy*. 2007;32:2902–2913.
27. Xu J, Froment G. Methane steam reforming, methanation and water-gas shift: I. Intrinsic kinetics. *AIChE J*. 1989;35:88–96.
28. Tsotsas E, Schlünder E. Heat transfer in packed beds with fluid flow: remarks on the meaning and the calculation of a heat transfer coefficient at the wall. *Chem Eng Sci*. 1990;45:819–837.
29. De Wasch A, Froment G. Heat transfer in packed beds. *Chem Eng Sci*. 1972;27:567–576.
30. Elnashaie S, Elshishini S. Modeling, Simulation and Optimization of Industrial Fixed Bed Catalytic Reactors. Topics in Chemical Engineering, Vol. 7. NY: Gordon and Breach Science Publisher, 1993.
31. Shu J, Grandjean B, Kaliaguine S. Methane steam reforming in asymmetric Pd and Pd-Ag porous SS membrane reactors. *Appl Catal A: General*. 1994;119:305–325.
32. Desideri U, Paolucci A. Performance modeling of a carbon dioxide removal system for power plants. *Energy Convers Manage*. 1999;40:1899–1915.
33. Uemiya S, Sato N, Ando H, Matsuda T, Eiichi K. Steam reforming of methane in a hydrogen-permeable membrane reactor. *Appl Catal*. 1991;67:223–230.
34. Tong J, Matsumura Y. Pure hydrogen production by methane steam reforming with hydrogen-permeable membrane reactor. *Catal Today*. 2006;111:147–152.
35. Tong J, Matsumura Y, Suda H, Haraya K. Experimental study of steam reforming of methane in a thin (6 μM) Pd-based membrane reactor. *Ind Eng Chem Res*. 2005;44:1454–1465.
36. Ewan BCR, Allen RWK. A figure of merit assessment of the routes to hydrogen. *Int J Hydrogen Energy*. 2005;30:809–819.
37. Chikazawa Y, Konomura M, Uchida S, Sato H. A feasibility study of a steam methane reforming hydrogen production plant with a sodium-cooled fast reactor. *Nucl Technol*. 2005;152:266–272.
38. Haeseldonckx D, D'haeseleer W. The use of the natural-gas pipeline infrastructure for hydrogen transport in a changing market structure. *Int J Hydrogen Energy*. 2007;32:1381–1386.
39. Pede G, Rossi E, Chiesa M, Ortenzi F. Test of blends of hydrogen and natural gas in a light duty vehicle. 2007 JSAE/SAE - International Fuels and Lubricants Meeting, July 2007.
40. Chiesa P, Lozza G, Mazzocchi L. Using hydrogen as gas turbine fuel. *ASME J Eng Gas Turbines Power*. 2005;127:73–80.

Manuscript received Oct. 5, 2007, and revision received Mar. 17, 2008.